ISSN 1063-7788, Physics of Atomic Nuclei, 2022, Vol. 85, No. 10, pp. 1–10. © Pleiades Publishing, Ltd., 2022.
Russian Text © The Author(s), 00000, published in Yadernaya Fizika i Inzhiniring, 00000, Vol. 00000, No. 00000, pp. 00000–00000.

Magnets of the SPASCHARM Experiment at the U-70 Accelerator Complex

A. P. Meshchanin[a,*], A. N. Vasil'ev[a,b], Yu. M. Goncharenko[a], V. A. Korotkov[a], N. G. Minaev[a], V. V. Mochalov[a,b], V. L. Rykov[b], A. D. Ryabov[a], T. D. Ryabova[a], A. V. Ryazantsev[a], P. A. Semenov[a,b], S. A. Semin[a], and Z. G. Simonova[a]

[a] *National Research Center Kurchatov Institute–Institute for High Energy Physics, Protvino, Moscow oblast, Russia*
[b] *National Research Nuclear University Moscow Engineering Physics Institute, Moscow, Russia*
**e-mail:* @@@

Received January 1, 2022; revised January 1, 2022; accepted January 1, 2022

Abstract—A system of four magnets is described, which is a part of the SPASCHARM experimental setup at the U-70 accelerator complex for the study of spin effects in hadron interactions. A unique magnet with a field of 2.4 T and a field uniformity at the level of 10 ... a working volume of 60 cm ... is used to pump and retain polarization in a polarized proton frozen target. A special wide-aperture magnet ... the central part of the spectrometer of the setup based on drift tubes. For precision guidance of the beam to the center of the target, two small correcting magnets developed by the Efremov Research Institute of Electrophysical Equipment were manufactured and introduced into the setup.

DOI: 10.1134/S1063778822100386

INTRODUCTION

The SPASCHARM polarization experiment [1] is being carried out at the U-70 accelerator complex in Protvino to study the spin structure of the nucleon and the spin dependence of the strong interaction at U-70 energies. The SPASCHARM experimental setup on a secondary beam of negative particles with a momentum of ~26.5 GeV/c is shown in Fig. 1.

The complex of the polarized proton target of the SPASCHARM experiment includes a Dinozavr magnet with a high field uniformity in the working volume of the target of 60 cm^3. It ensures the operation of the polarized target, which is a critically important subsystem of the SPASCHARM experiment.

The front universal wide-aperture spectrometer is intended to simultaneously detect all secondary particles in the forward hemisphere of interactions

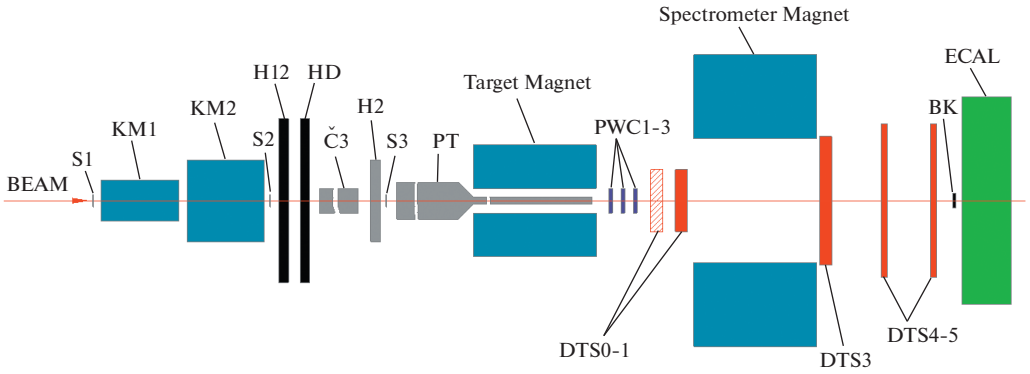

Fig. 1. The layout of the SPASCHARM setup on channel no. 14 of the U-70 accelerator complex. S1, S2, S3, beam scintillation counters; KM1, KM2, corrective magnets of the SP-140 type; H12, beam hodoscopes X and Y; HD, precision beam hodoscopes X and Y; C3, third threshold Cherenkov counter (the first two, C1 and C2, are not shown in the figure, they are far to the left); H2, beam hodoscope; RT, polarized target ZPPM-200M; Target Magnet, Dinozavr magnet of the polarized target; PWC1-3, block of proportional chambers; DTS0-1, small drift chambers; Spectrometer Magnet, SPASCHARM wide-aperture magnet; DTS3, DTS4-5, large drift chambers; BK, beam counter; ECAL, electromagnetic ... imeter ChSPP-720 based on TF1-000 lead glasses.

(according to the Feynman variable $x_F > 0.3$) up to transverse momenta of 2 GeV/c. Hence, it follows that the angular acceptance of the experimental setup for a beam with a momentum of 26.5 GeV/c should be on the order of ±110 mrad. In this case, the spectrometer implements a complete geometry in the azimuthal angle, which allows measuring spin asymmetries with extremely low systematic errors. Measurement and intercomparison of polarization effects for a large set of different reactions in a wide kinematic range is fundamentally important for revealing the role of spin in the most difficult to understand nonperturbative region of strong interactions. The SPASCHARM spectrometric magnet is the central part of the front wide-aperture spectrometer.

For accurate guidance of the beam at the center of the target, the setup includes two corrective magnets designed from the blueprints of the Efremov Research Institute of Electrophysical Equipment; these magnets are used in the particle channels of the U-70 accelerator complex [2]. The four magnets of the SPASCHARM experiment are thoroughly described in this paper.

1. THE COMPACT DINOZAVR ELECTROMAGNET FOR A "FROZEN" POLARIZED PROTON TARGET

The polarization in the ZPPM-200M target is obtained ("pumped") in the magnetic field transverse to the beam of the Dinozavr electromagnet with warm windings [3]. It is a further development of the original project of the Dzhin magnet [4], which for many years provided the operation of a polarized target in the PROZA [5] and PROZA-M [6] experiments. The general appearance of the Dinozavr magnet is shown in Fig. 2.

The ZPPM-200M target is placed in the center of the magnet's working gap. The field in the gap is formed by poles of permendur 49KF with a width of 164 mm, a length of 1000 mm, and a thickness of 80 mm. The field flux is closed through magnetic circuits made of steel grade St.3.

Proton polarization pumping is based on the effect of excitation of electron paramagnetic resonance (EPR) with polarization of atomic electrons in the magnetic field and subsequent transfer of polarization to protons through a chain of atomic transitions [5].

The resonant frequency of the EPR depends on the induction of the magnetic field. The microwave generator we have at our disposal covers the frequency range from 66.17 to 67.17 GHz. For EPR, this corresponds to an induction from 2.365 to 2.401 T, which is necessary for successful pumping of the proton polarization in the target. On this basis, the working field of the Dinozavr magnet in the polarization pumping mode was chosen to be 2.4 T.

The upper and lower magnetic circuits, together with the poles, can be symmetrically pulled together or apart using a power movement system, which consists of a 5 kW electric motor, a two-stage worm gear, and a chain drive. The total transmission coefficient of the power system is 700. The load-bearing power structures consist of two steel plates 50-mm thick fastened with four racks.

In a pulled-together state, with a gap height between the poles of 75 mm and a rated magnet supply current of 1440 A, the field reaches 2.4 T in its central part. In this mode, the proton polarization is pumped for 4–6 h in the target cooled to a temperature of approximately 0.2–0.3 K. Further, after the target is cooled by another order of magnitude (to ~0.03 K), the procedure for spreading the poles apart to 250 mm begins, opening the magnet aperture for secondary particles emitted from the target within ±300 mrad horizontally and ±250 mrad vertically. At the beginning of the pole-spreading procedure, the field in the working gap is reduced to 0.65 T, so as not to deal with the full force of attraction between the two halves of the magnet (which is approximately 40–50 tons at 2.4 T) and thereby not damage the spreading mechanism. Further, the upper and lower halves of the magnet are pulled apart in several steps with a simultaneous gradual increase of the supply current so that the magnetic induction in the target zone never drops below ~0.4 T. Upon completion of this separation phase, which takes 10–15 min, the magnet supply current again reaches its rated value of 1440 A and the field in the target zone is ~0.4 T. The polarization of the target is maintained in this field for the time of collecting statistics on the beam (1–2 days).

For successful pumping of proton polarization over the entire working volume of the target, it is necessary that the inhomogeneity of the magnetic field inside this volume does not exceed the natural width of the absorption line of the nuclear magnetic resonance signal in an ideally uniform field. This width depends on the dipole–dipole interaction of protons in the target material the structure of this material [7]. In pentanol $C_5H_{12}O$ with the addition of the TEMPO radical, which is currently used as a working substance, the relative absorption line width (RMS) in a field of 2.4 T is approximately ~1.65×10^{-4}. It is a complicated task to build a warm magnet with ferromagnetic poles that provides such a high field uniformity at its magnitude close to saturation of the poles. At the design stage of the magnet, numerous calculations were carried out [8] in order to optimize its parameters.

A design with two main and two forming windings was chosen. Two main coils are built into the magnetic circuits; each coil consists of 5 sections (5 × 8 turns); these are made of a 8 × 8 mm^2 copper tube with an inner diameter of 4.5 mm for demineralized water. The forming windings, which partially fill the interpolar space and leave a free aperture 80 mm wide, consist of

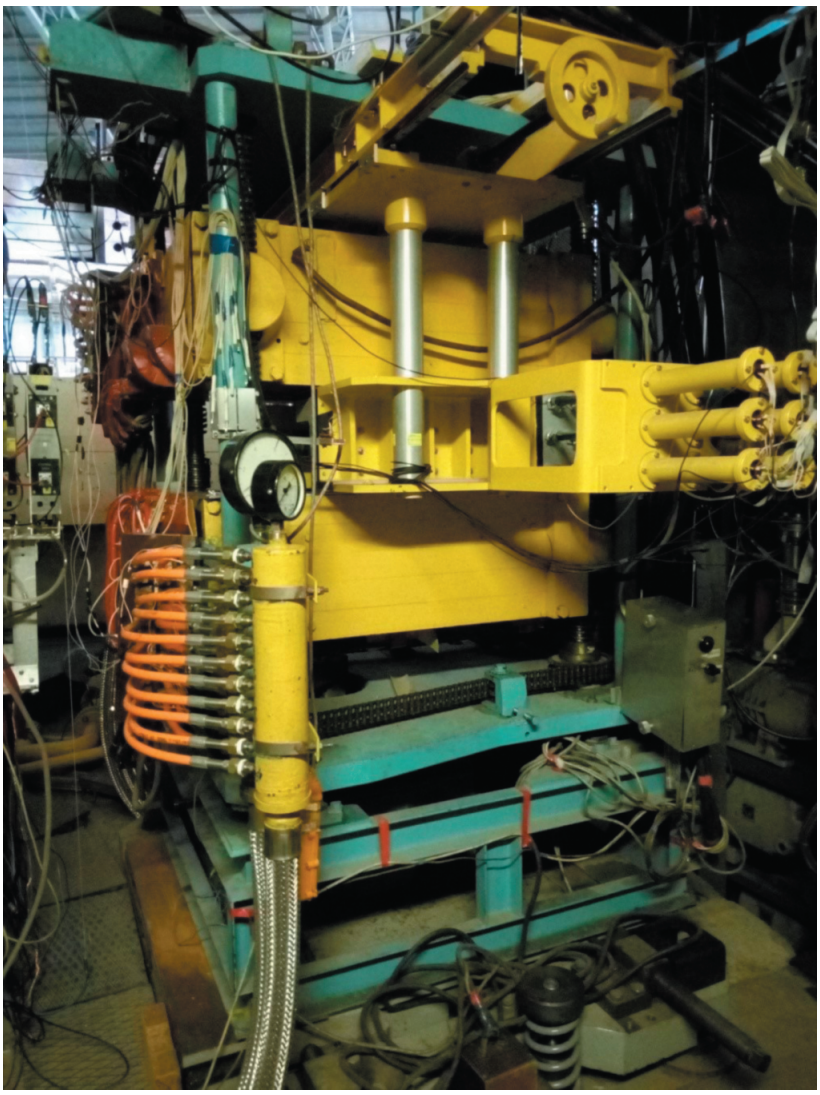

Fig. 2. The general form of the Dinozavr magnet with the veto system in the working position and working communications at the SPASCHARM setup on channel no. 25 of the U-70 accelerator complex.

three sections (3 × 5 turns). The total number of turns in the winding is 110. Electrically, all sections are connected in series and water-wise, in parallel. To form a field with good uniformity, it was also necessary to place triangular steel shims in the corners of the aperture along the entire length of the poles; the shims were glued to the poles with epoxy resin.

As a result, in the central part of the magnet in a cylinder with a diameter of 20 mm and a length of 200 mm, a uniform field was obtained with an induction of 2.4 T, the highest relative minimum-to-maximum variation of 13×10^{-4} and a standard deviation from a constant volume of 4.3×10^{-4}. The topography of the relative deviations of the resulting field on the target's surface from its average value over the volume, $\langle B \rangle$, is illustrated in Fig. 3 on the left.

However, such deviations from homogeneity were still too large for work with a polarized target. The reason for this is not only the final accuracy of the mechanical manufacture of magnet parts and their assembly. The uncertainty in the magnetic characteristics of the ferromagnetic materials and their variation from sample to sample and even within the same structural element is a serious problem in saturation mode. In order to improve the quality of the field, additional shimming in the magnet aperture was undertaken. As a result, the field pattern noticeably improved, which is shown in Fig. 3 on the right. The maximum relative variation in this field is $\sim\pm 4 \times 10^{-4}$ and the standard deviation from the constant in volume is $\sim\pm 1.3 \times 10^{-4}$, which fits rather well into the allowable inhomogeneity $\sim\pm 1.65 \times 10^{-4}$ (see above). The evidence of the successful shimming is that a sta-

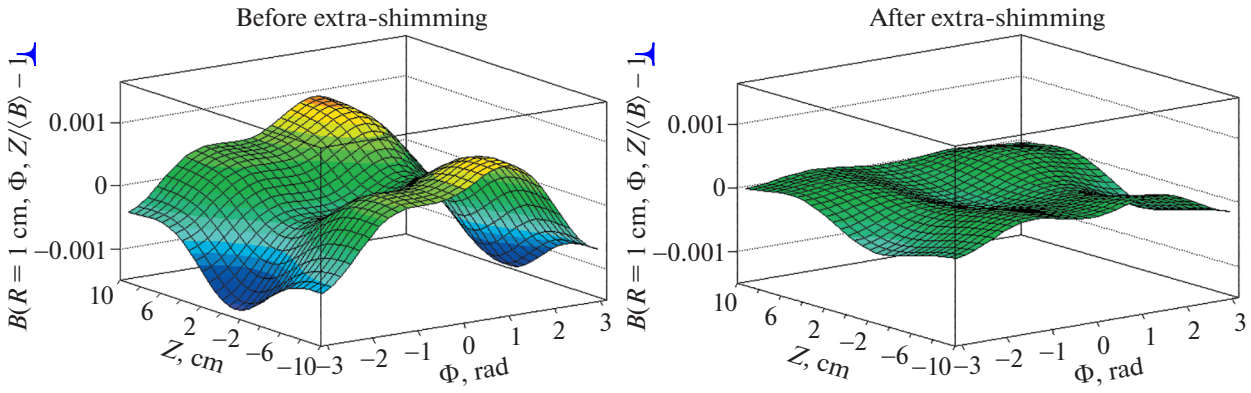

Fig. 3. The relative variations ~~in~~ the magnetic field ~~on~~ the surface of a cylinder ~~with a~~ 20 mm diameter and 200 mm length. Left: before extra shimming; right: after shimming.

ble polarization of protons in the pentanol target up to 75% was obtained in such a field and ~~a session on collecting statistics on the beam was~~ successfully carried out at this polarization.

In conclusion, we list some technical characteristics of the ~~Dinozavr~~ magnet that were not mentioned in the ~~text~~:

• The electrical voltage ~~on the winding at a rated~~ current of 1440 A is 207 V.

• The magnet cooling system is designed for demineralized water at a pressure drop of 20 atm. The inlet water temperature should not exceed 30°C. The total water consumption under these conditions is 8 ~~m^3/h~~.

The electromagnet is powered using a 28TP2 thyristor power supply (U_{rate} = 215 V, I_{rate} = 1500 A). The thyristor converter is based on the 3-phase Larionov symmetrical bridge circuit. A passive L-shaped LC filter is used to suppress rectified voltage pulsations.

Considering the specific nature of the disturbances acting on the system, which can be arbitrarily divided into high-frequency oscillations of the ~~supply~~ network and low-frequency oscillations, including heating of the load, a double-circuit structure of the thyristor converter control system was chosen. This is ensured by its division into a fast-acting voltage stabilization circuit and a slow-acting current circuit, which allows a high degree of stabilization to be obtained with a relatively simple correction.

The ~~mode~~ of polarization ~~pumping~~ in the target has ~~severe~~ restrictions on the field fluctuations ~~(~~no more than ~$\pm 1.5 \times 10^{-4}$~~)~~, which ~~is~~ the same as the requirements ~~for~~ field uniformity. The permissible value of the field pulsations in all modes is also limited by the thermal load from eddy currents on the dissolution chamber ~~in~~ the refrigerator. At operating temperatures of 30 mK, it should not exceed 100 mW. Estimates show ~~that~~ at a frequency of 300 Hz~~,~~ which is the main frequency in the spectrum of 6-pulse thyristor converters, this corresponds to a limit on the field pulsation amplitude of no more than 0.25 mT in the polarization retaining mode.

Figure 4 shows the dependence of the induction $B(I)$ on the supply current I at the center of the working region of the ~~Dinozavr~~ magnet with a closed yoke.

2. A WIDE-APERTURE SPECTROMETRIC MAGNET OF SPASCHARM

For momentum analysis of charged ~~particles~~ the SPASCHARM experiment uses ~~a large~~ magnet (see Fig. 5) with ~~an~~ aperture of $X \times Y = 2.3 \times 1$ m^2, which ensures the detection of secondary particles by the system of all track detectors in the angular range up to ~$\pm$110 mrad vertically and, potentially, up to ~$\pm$240 mrad ~~horizontally~~; this reliably exceeds the requirements for the angular acceptance of the spectrometer with regard to the goals of the physical program of the experiment.

This magnet, which was originally C-shaped, with a magnetic field of 1 T at a vertical gap of 1 m, was constructed in the mid-1980s for the NEPTUNE experiment [9] at the UNK collider [10]. To ~~work as part of~~ the SPASCHARM experiment, the magnet was significantly modernized, namely, the yoke was modified to a ~~W~~-shape using 30% of the previous yoke, changes were made to the magnet ~~winding~~, and new screens ~~were made~~ to protect the track detectors from the scattered magnetic field. ~~To~~ optimize the geometry, including the location of the protective screens, the choice of optimal power supply modes for the magnet, etc., detailed numerical calculations of the magnetic field ~~were~~ carried out for a large number of options. ~~Precision~~ measurements of the field topography in the working aperture of the magnet with an accuracy of ~(0.1–0.3)% ~~were also made~~.

A predominantly vertical magnetic field is formed in the aperture of the SPASCHARM spectrometric magnet by two steel poles with dimensions $X \times Z$ = 800 × 1000 mm^2. The magnetic flux is closed through

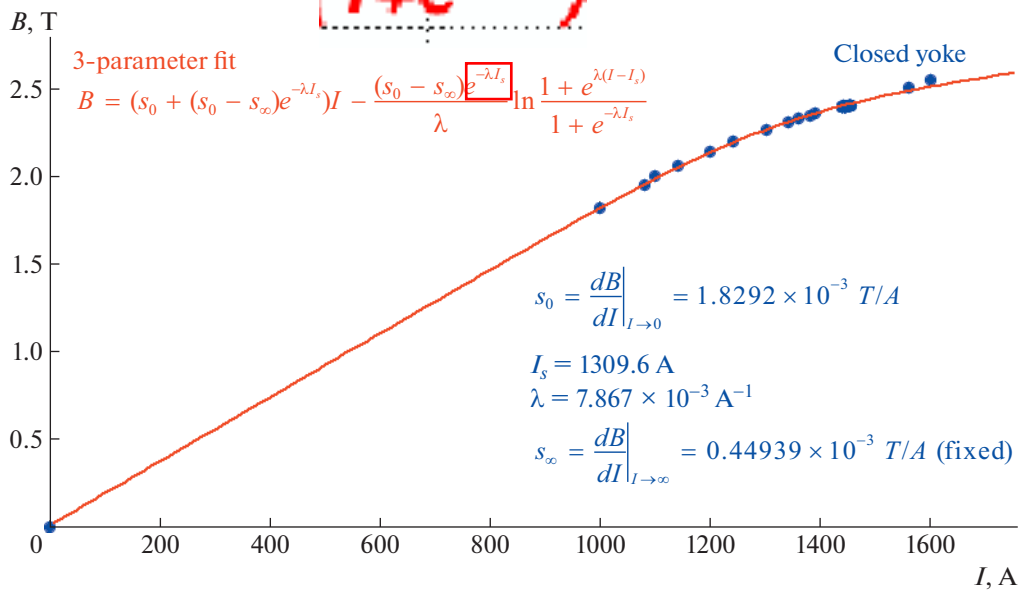

Fig. 4. The induction $B(I)$ ~~in~~ the center of ~~the Dinozavr magnet~~ as a function of the ~~supply~~ current ~~with a closed yoke~~.

two symmetrical branches of the steel yoke with a cross section of 850 × 1000 mm^2 each. The ~~winding~~ of the magnet consists of two sections: upper and lower, each with 256 turns. In the present configuration, the sections are connected to the power supply in parallel. The magnet has the following operating parameters:

- The operating current is ~~2000~~ A/~~turn~~;
- The conductor is a copper tube with a square ~~section~~ of 16.5 × 16.5 mm^2 and an internal ~~hole with~~ a diameter ~~of~~ 10 mm for cooling water;
- The resistance of one ~~winding~~ section is 0.105 Ohm;
- The ~~restriction~~ on the specific resistance of the cooling water is ~~no~~ less than 10 000 Ohm cm;
- The cooling water pressure drop ~~across~~ the ~~winding~~ is 20 atm;
- The magnet weight is 150 tons.

The magnet is powered by a generator 1GP-550-750 (U_{rate} = 150 V, I_{rate} = 3670 A) of a 10AP electric machine converter unit. The stabilization of the current through the load is carried out by a current feedback circuit acting on the control system of a low-power thyristor converter of the generator excitation ($U_{excit.max}$ = 250 V, $I_{excit.max}$ = 13.2 A).

The calculated dependence of the field induction in the center of the magnet versus the supply current is shown in Fig. 6.

Currently, due to power supply limitations, the magnet is operated at a reduced current of 1 kA/turn. To remove the heat generated during the operation of the magnet, demineralized cold water is pumped through the ~~winding~~ with an inlet temperature no higher than 30°C under a pressure of 11 atm. The water temperature at the outlet of the ~~magnet~~ usually does not exceed 50°C.

The magnet is positioned so that its center is 3.26 m ~~down~~ the beam from the center of the polarized target. In this case, approximately 1.5 m remains for placing track detectors between two magnets in the region of a ~~weakened~~ magnetic field. ~~A~~ 100-mm-thick steel screen with ~~a window~~ $X \times Y = 2.3 \times 0.7$ m^2 is ~~placed~~ at ~~a~~ distance of ~0.85 m ~~up~~ the beam from the center of ~~the~~ magnet ~~to~~ protect the track detectors from the scattered magnetic field. For the same purpose, a double screen of two iron sheets, which are 50-mm thick each, with a much larger window, $X \times Y = 2.3 \times 1.5$ m^2, ~~was~~ installed ~~down~~ the beam at ~~a~~ distance of ~1.7 m from the center of the magnet.

The magnetic field in a magnet with ~~this~~ geometry is obviously far from uniform, ~~as~~ illustrated by some ~~of the~~ distributions in Fig. 7.

To use the magnet for charged particle tracking, ~~detailed~~ measurements of the field topography ~~were~~ carried out ~~by a~~ system of Hall sensors [11] in ~~a~~ volume ~~with~~ dimensions $X \times Y \times Z = 1.24 \times 0.84 \times 1.96$ m^3. All three field components were measured at 34 496 points on the grid with a step of 4 cm for each of the coordinates. The Hall sensors ~~were calibrated~~ in the induction range of ±0.8 T ~~using an~~ NMR magnetometer [12] ~~with an accuracy of ~(0.4–0.6) mT~~. During the field topography measurements, the full cycle of which took ~10 h, the ~~"floating"~~ of the ~~supply~~ current and ~~the~~ field in the magnet did not exceed ±0.01%. Variations ~~were~~ monitored by a current monitor and two NMR sensors fixed on the poles.

The measurements covered a significant part of the working volume of the magnet, but, unfortunately, not

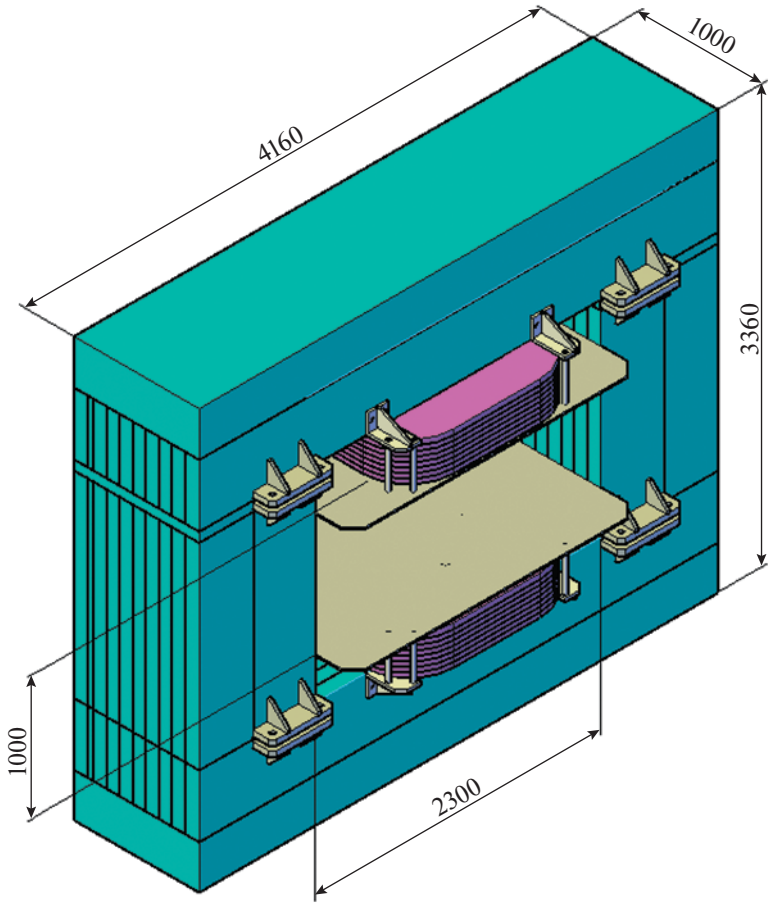

Fig. 5. The general view of the W-shaped yoke of the SPASCHARM magnet.

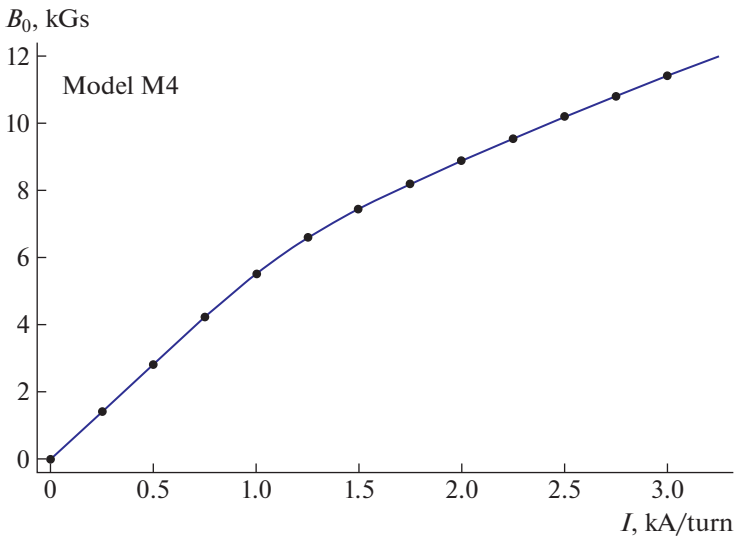

Fig. 6. The calculated dependence of the magnetic induction in the center of the magnet on the current per winding turn.

the entire volume. Due to the specific design features of the magnet and the limitations of the system for moving the Hall sensors [11], it was not possible to make measurements at distances more than 0.4 m from the center of the magnet up the beam, as well as near the aperture boundaries. For this reason, the

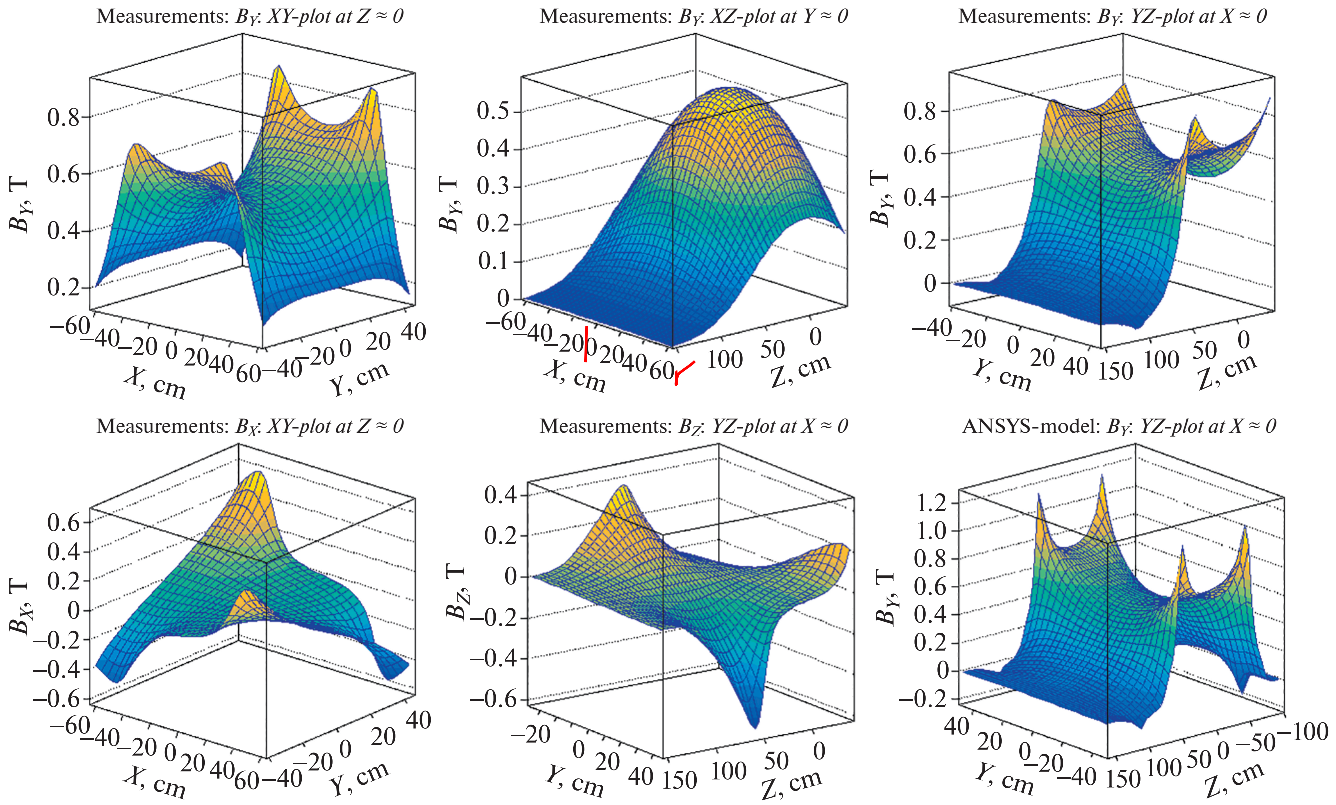

Fig. 7. Some distributions of the field in the aperture of the magnet in planes passing through its center. Five out of the 6 distributions are taken from measurements, and the sixth in the bottom right corner is the result of numerical simulation [1] using the ANSYS program.

analysis of data for tracing charged particles in a magnet currently uses the calculated field pattern compared against magnetic measurements. The root mean square deviation (RMS) of the calculations and measurements for all 101 920 measured values of all three field components was found to be ±1.9 mT, which is ±0.35% of the field at the center of the magnet.

The positioning error of the sensors near the edges and corners of the poles, where the induction gradients are very large and reach ~5 mT/mm, significantly contribute to the deviations over the entire volume. If we limit ourselves to the region far from the magnet poles ($|Y| < 30$ cm), here RMS = ±0.95 mT = ±0.18% from the field at the center of the magnet. In the absolute normalization, on average over the volume, the calculated and measured magnetic inductions nearly coincide: the difference is ~0.13% with the error of the comparison procedure estimated at ±0.15%.

Some illustrations for the comparison of calculations and measurements are presented in Fig. 8 in terms of field integrals along the Z axis. The figure shows only two transverse components that make a dominant contribution to the deflection of charged particles flying at small angles to the Z axis in the magnet. In the root-mean-square deviations from zero for the entire XY plane, there is agreement within ~±0.3% for the integral of B_X and ~±0.18% for the integral of B_Y. Far from the poles (at $|Y| < 30$ cm), the agreement is no worse than ~±0.14% for both components.

The measured induction at the center of the magnet is 0.5398 ± 0.0004 T, and the field integral along the magnet axis is 0.703 ± 0.001 T m. Hence, the effective length is ~1.3 m. The scattered field reaches approximately 15–17 mT in the zone of the nearest track detector up the beam and 0.2 mT in the zone of the nearest detector down the beam.

3. THE KM1 AND KM2 CORRECTING BEAM MAGNETS

The SP-140 Electromagnet correctors were designed at the Efremov Research Institute of Electrophysical Equipment in 1968 (blueprint no. OA502738). In accordance with this blueprint, two identical magnets were manufactured under production conditions at the Institute for High Energy Physics for the SPASCHARM setup (see Fig. 9) for precision guidance of the beam to the center of the polarized target.

The magnet dimensions are 662 × 630 × 310 mm^3; their weight is 380 kgf. At a working magnet current of 9 A in its working aperture with a height of 100 mm and width of 200 mm, the magnetic field reaches 0.1 T.

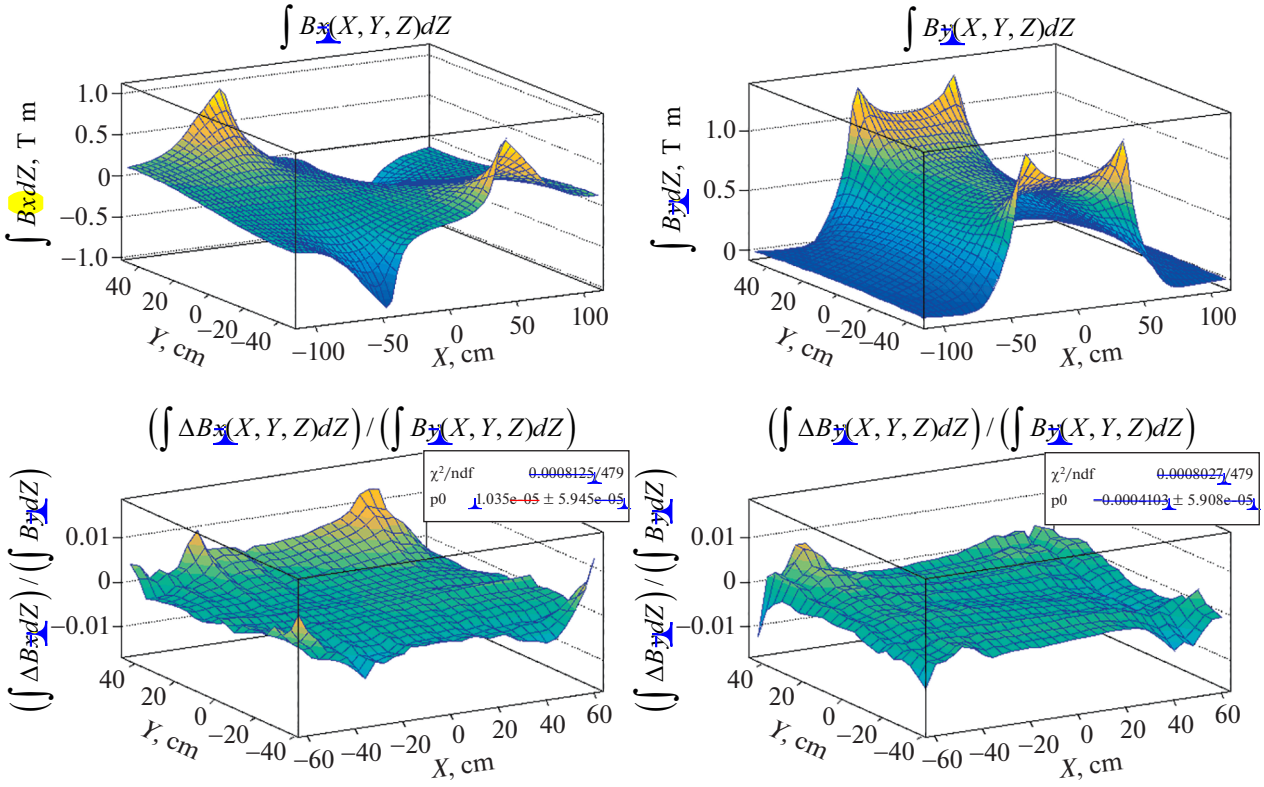

Fig. 8. An illustration of the degree of agreement between the calculations [1] and measurements in integrals along the Z axis (parallel to the beam) with respect to the transverse field components B_X and B_Y. Top row: calculated distributions of integrals in the transverse X–Y plane for the full working volume of the magnet. Bottom row: relative differences between the calculated and measured integrals normalized to the integrals of the principal component B_Y for the part of the working volume where the measurements were made. Notation: $\Delta B(X, Y, Z) = B_{\text{calc}}(X, Y, Z) - B_{\text{meas}}(X, Y, Z)$. In the bottom row, the numbers in the stat-boxes correspond to the fitting by a constant with unit errors of 2D distributions in the band $|Y| < 30$ cm.

The aperture dimensions were chosen so that the beam completely fits it in the zone where the corrector magnets were placed. The length of the magnet along the iron poles is 500 mm. By varying the excitation current of the windings, it is possible to aim the center of the particle beam at the center of the polarized target ZPPM-200M with an accuracy no worse than 0.3 mm. The beam size (full width at half height) in the target with a diameter of 20 mm is 7 mm.

The winding of the SP-140 magnet consists of four coils connected in series. The number of turns in the winding is 2240, the average length of a turn is 1.3 m, the conductor is a PSD wire. The winding resistance at 15°C is 8.4 Ohm, the inductance of the electromagnet assembly is 4.4 H, the winding is cooled by natural air, the maximum overheating of the winding copper is 65°C.

Figures 10 and 11 show some results of measuring the magnetic field of the SP-140 magnet using a Hall sensor. It can be seen that the field is linear in current up to 12.5 A and uniform in length up to 200 mm from the center of the magnet.

Currently, rectifiers of the VU-110/24A type are used as power sources for the magnets; at a network voltage of 220/380 V they produce a rectified voltage of 110 V and a current of 24 A at the output. The weight of the rectifier is 60 kg.

CONCLUSIONS

The electromagnets of the SPASCHARM experiment presented in this paper are an organic part of the physical setup and perform the following functions:

• A dinozavr magnet with an induction of 2.4 T at a magnetic field uniformity of ~±0.013% in the working volume of the target of 60 cm^3 provides the proton polarization pumping up to 75%, followed by sustaining the polarization for 1–2 days;

• The wide-aperture SPASCHARM magnet provides simultaneous measurement of momenta with an accuracy potentially up to ~±(0.1–0.3)% for all charged secondary particles in the forward hemisphere of interactions (in the Feynman variable $x_F >$ 0.3) up to transverse momenta of 2 GeV/c with uninterrupted 2π coverage over the azimuth angle within the

Fig. 9. The ~~general form of the location~~ of the KM1 and KM2 ~~corrective magnets~~ ~~on channel~~ no. 14 of U-70.

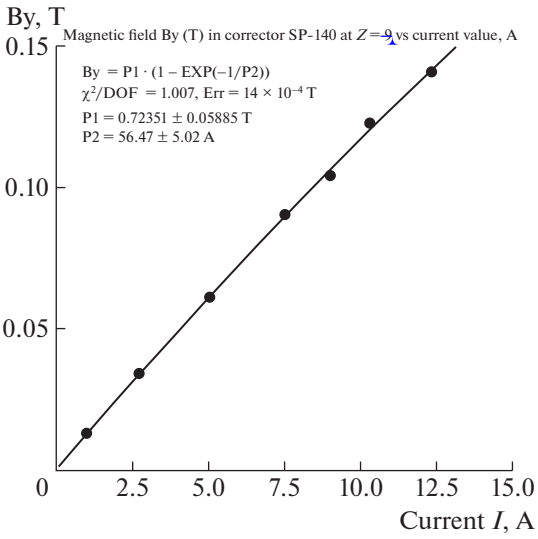

Fig. 10. The induction $B_y(I)$ in the center of the SP-140 magnet as a function of the ~~supply~~ current I.

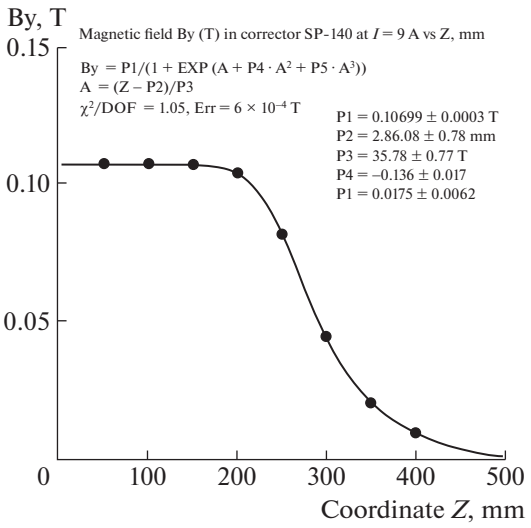

Fig. 11. The induction $B_y(I)$ ~~at the center~~ of the SP-140 magnet ~~along the central axis~~.

acceptance of the setup, which minimizes systematic errors in measurements of spin effects;

• Precise ~~guidance~~ of the ~~particle~~ beam ~~in the channel~~ to the center of ~~the~~ polarized target is performed by the KM1 and KM2 ~~corrective magnets~~.

~~During~~ a number of ~~sessions of work on the beam~~, the magnets described here showed ~~good~~ reliability ~~of operation~~ and stability of parameters. They are intended to be used ~~in the program of~~ the SPASCHARM experiment at the U-70 accelerator ~~complex for the next~~ decade.

FUNDING

The study was carried out at the National Research Center Kurchatov Institute–Institute for High Energy Physics with the financial support of the Russian Science Foundation (grant no. 22-12-00164) and partial financial support from the Ministry of Higher Education and Science (Priority-2030 Program at the National Research Nuclear University MEPhI).

CONFLICT OF INTEREST

The authors declare that they have no conflicts of interest.

REFERENCES

1. V. V. Abramov et al., IHEPh Preprint 2019-12 (Inst. High Energy Phys., Protvino, 2019).
2. E. D. Bondarenko et al., IHEPh Preprint 90-58 (Inst. High Energy Phys., Protvino, 1990).
3. O. A. Grachev et al., Prib. Tekh. Eksp., No. 3, 189 (1993).
4. M. M. Burkhin et al., Prib. Tekh. Eksp., No. 1, 30 (1981).
5. I. A. Avvakumov et al., IHEPh Preprint 81-15 (Inst. High Energy Phys., Serpukhov, 1981).
6. V. D. Apokin, N. I. Belikov, A. N. Vasil'ev, Yu. M. Goncharenko, O. A. Grachev, V. N. Grishin, A. M. Davidenko, A. A. Derevshchikov, Yu. A. Il'in, V. A. Kormilitsyn, Yu. A. Matulenko, V. A. Medvedev, Yu. M. Mel'nik, A. P. Meshchanin, et al., Instrum. Exp. Tech. **41**, 464 (1998).
7. V. N. Alferov et al., Prib. Tekh. Eksp., No. 3, 157 (2019).
8. A. G. Daikovskii and Yu. I. Portugalov, IHEPh Preprint 78-68 (Inst. High Energy Phys., Serpukhov, 1978).
9. V. L. Solovianov, in *Proceedings of Workshop on the Experimental Program at UNK* (Protvino, 1988), p. 191.
10. IHEPh Preprint 93-27 (Inst. High Energy Phys., Protvino, 1993).
11. A. Abragam, *The Principles of Nuclear Magnetism* (Clarendon, Oxford, 1961), Chap. 4.
12. G. V. Karpov et al., INPh Preprint No. 2004-55 (Inst. Nucl. Phys. Sib. Branch of RAS, Novosibirsk, 2004).

Translated by M. Chubarova

SPELL OK